Limitations on Lightwave Communications Imposed by Optical-Fiber Nonlinearities

ANDREW R. CHRAPLYVY

(Invited Paper)

Abstract—This paper describes optical nonlinearities in the context of lightwave systems limitations. The nature and severity of system degradation due to stimulated Raman scattering, carrier-induced phase noise, stimulated Brillouin scattering, and four-photon mixing will be discussed. In particular, the system power limitations will be plotted as a function of number of wavelength-multiplexed channels. Methods for scaling these results with changes in system parameters will be presented.

I. INTRODUCTION

THE attractiveness of lightwave communications is the ability of silica-optical fibers to carry large amounts of information over long repeaterless spans. To utilize the available bandwidth, numerous channels at different wavelengths can be multiplexed on the same fiber. To increase system margins, higher transmitter powers or lower fiber losses are required. All these attempts to fully utilize the capabilities of silica fibers will ultimately be limited by nonlinear interactions between the information-bearing lightwaves and the transmission medium. These optical nonlinearities can lead to interference, distortion, and excess attenuation of the optical signals, resulting in system degradations.

There exists a rich collection of nonlinear optical effects in fused silica fibers, each of which manifests itself in a unique way. Stimulated Raman scattering, an interaction between light and vibrations of silica molecules, causes frequency conversion of light and results in excess attenuation of short-wavelength channels in wavelength-multiplexed systems. Stimulated Brillouin scattering, an interaction between light and sound waves in the fiber, causes frequency conversion and reversal of the propagation direction of light. Cross-phase modulation is an interaction, via the nonlinear refractive index, between the intensity of one light wave and the optical phase of other light waves. Four-photon mixing is analogous to third-order intermodulation distortion whereby two or more optical waves at different wavelengths mix to produce new optical waves at other wavelengths.

Each of these nonlinearities will affect specific lightwave systems in different ways. However, in general, stimulated Raman scattering, stimulated Brillouin scatter-

ing, and four-photon mixing will deplete certain optical waves and, by means of frequency conversion, will generate interfering signals for other channels. These will degrade both direct detection and heterodyne systems. Cross-phase modulation, on the other hand, affects only the phase of optical signals. Consequently only angle-modulated systems will be affected by this nonlinearity.

This paper describes optical nonlinearities in the context of lightwave system limitations. The four nonlinearities mentioned above will be discussed and the nature and severity of system degradation caused by each nonlinearity will be described. In particular, the system power limitations will be plotted as a function of number of optical channels. Methods for scaling these results with changes in system parameters such as fiber loss, core diameter and length will be discussed.

II. NONLINEAR GAIN AND SYSTEM PARAMETERS

Most nonlinear optical interactions involving two overlapping optical waves propagating in a medium can be characterized generally by

$$P_1(L) = P_1(O) \exp(gP_2L/A) \qquad (1)$$

where $P_1(O)$ and $P_1(L)$ is the power of one wave entering and exiting, respectively, a medium of length L. This amplified wave is commonly called the probe wave. P_2 is the injected power of the other wave, called the pump, which generates the gain for the first wave. The cross-sectional area common to the light beams is A; the gain coefficient g (expressed in centimeter per Watt) is a direct measure of the strength of the nonlinearity. Equation (1) assumes that P_2 is constant throughout the nonlinear medium, that is, there is no pump depletion due to the nonlinearity and no intrinsic loss. Furthermore, (1) assumes that the polarization states of the pump and probe waves are the same. Neither of these assumptions typically hold in fibers. Attenuation in long fibers is not negligible and the polarization states of the pump and probe waves can evolve differently in the fiber. Consequently, (1) must be modified to be applicable to single-mode optical fibers [1]. The correct expression is

$$P_1(L) = P_1(O) \exp(gL_eP_2/bA_e) \qquad (2)$$

where P_2, $P_1(O)$, $P_1(L)$, and g are defined as before. The effective area of the propagating waves A_e is evaluated by

calculating the average modal overlap between the pump and probe waves [2]-[4]. However, in general, if the pump and probe wavelengths are comparable and both are slightly longer than the fiber cutoff wavelength, then $A_e \approx A$, where A is the core area of the fiber [5]. The effective fiber length L_e replaces the actual length L in order to account for the exponential decay with length of the pump power due to fiber loss. A simple integration shows that

$$L_e = \frac{1 - e^{-\alpha L}}{\alpha} \qquad (3)$$

where α is the loss coefficient of the fiber. For $\alpha L \ll 1$, $L_e \approx L$; for $\alpha L \gg 1$, $L \approx 1/\alpha$. The factor b accounts for the relative polarizations of pump and probe waves and the polarization properties of the fiber. In a polarization-maintaining fiber, with identical pump and probe polarization states, $b = 1$. In a conventional fiber that does not maintain polarization, $b = 2$, which will be assumed in what follows.

Equation (2) describes the strength of optical nonlinearities as a function of system parameters. As a starting point, a long-haul ($L > 30$ km) single-mode system operating at 1.55 μm is assumed. The fiber is assumed to have a core area of 5×10^{-7} cm^2 (core diameter = 8 μm), a loss of 0.2 dB/km, and a chromatic dispersion of 16 ps/nm · km at $\lambda = 1.55$ μm. For operation in a densely packed frequency-multiplexed mode, channel spacing of 10 GHz is assumed. System limitations using these parameters will be discussed for the various nonlinearities. Also, the dependence of nonlinear effects on changes in system parameters will be described.

III. STIMULATED RAMAN SCATTERING

Raman scattering describes the parametric interaction of light with molecular vibrations. Incident light scattered by molecules experiences a downshift in optical frequency. The change in optical frequency is just the molecular-vibrational frequency (called the Stokes frequency). The details of Raman scattering are not important in this paper and can be found in numerous references [6]-[9]. The important point is that if two optical waves separated by the Stokes frequency are coinjected into a Raman-active medium, the lower frequency (probe) wave will experience optical gain generated by, and at the expense of, the higher frequency (pump) wave. This gain process is called stimulated Raman scattering (SRS) and can be described in fibers by (2). Because fused silica is a glass there is, in fact, a continuum of Stokes frequencies [10], corresponding to a spectral dependence of the gain coefficient g (in (2)) as shown in Fig. 1 [11]. (1 cm^{-1} = 30 GHz.) Note that the gain coefficient increases approximately linearly with pump-probe frequency separation up to a separation of about 500 cm^{-1}. This means that any channels separated by up to 15 000 GHz will be coupled via SRS. The magnitude of the gain coefficient shown in Fig. 1 is for a pump wavelength of 1 μm. The gain coef-
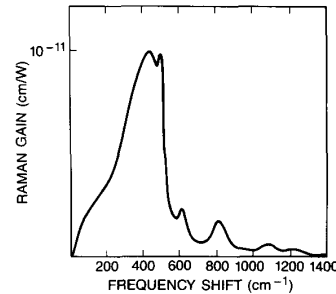

Fig. 1. Raman gain coefficient g versus frequency shift for fused silica at a pump wavelength of 1.0 μm. The gain coefficient scales inversely with pump wavelength [13]. 1 cm^{-1} = 30 GHz.

ficient scales inversely with wavelength [11] so that at 1.55 μm, which is the wavelength region under consideration, the peak Raman gain coefficient is about 7×10^{-12} cm/W.

In a single-channel lightwave system only one wavelength of light is injected into the fiber. However, this signal generates spontaneous Raman-scattered light which can then be amplified. It has been shown both theoretically [1], [12], [13] and experimentally [14]-[16] that amplification of Raman-scattered light will cause severe degradation (50% signal depletion) when

$$gL_e P/bA_e = 16. \qquad (4)$$

For the assumed system parameters, the injected signal power required to produce system degradation is about 1 W. It is clear that SRS will not be a factor in single-channel silica-fiber-based lightwave systems.

In wavelength-multiplexed systems the situation is quite different because channels at numerous wavelengths are injected into the fiber and the signals at longer wavelengths will be amplified by the shorter wavelength signals. In other words, the probe photons no longer build up from spontaneous Raman noise but are injected in macroscopic quantities as signal channels. This leads to system degradation at lower optical powers than in the single-channel case.

The degradation due to SRS for a two-channel system is schematically shown in Fig. 2 [17]. Suppose channel 1 and channel 2 are spaced such that SRS couples the two channels. This assumption will usually be satisfied in the 1.5-μm region because the broad stimulated Raman gain profile of silica (Fig. 1) will couple channels that are separated in wavelength by up to 100 nm.

Let channel 1 (pump) operate at a wavelength λ_1, which is shorter than λ_2, the wavelength of channel 2 (probe). Assume initially that both channels have equal optical power injected into the fiber. Suppose that in a return-to-zero (RZ) modulation format the bit pattern of the two channels is shown in Fig. 2(a). Schematically, the effect of SRS is to produce bit patterns as shown in Fig. 2(b). Thus far we have ignored the effects of dispersion. Note that whenever there is a mark in both channels the pump channel (λ_1) is depleted and the probe channel (λ_2) is amplified. If a space (zero light intensity) appears in either
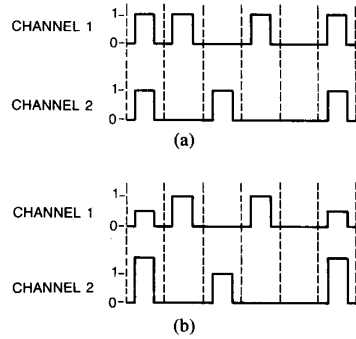
Fig. 2. (a) Bit pattern in two-channel wavelength-multiplexed system with no stimulated Raman interaction between channels. (b) Bit pattern with SRS ($\lambda_1 < \lambda_2$).

Fig. 3. Maximum power per channel versus number of channels which ensures SRS degradation below 1 dB for all channels.

channel, no intensity change occurs. (In conventional crosstalk a mark in channel 1 can produce a signal in channel 2 even if there is no mark in channel 2.) Furthermore, the effects of SRS on the two channels are not symmetric. Channel 1 experiences a partial closing of the eye pattern due to the depletion of individual bits, and therefore a degradation in signal-to-noise ratio. The opening of the eye in channel 2 is, in principle, unaffected because in the worst case some of the bits are amplified while the rest of the bits are unaltered. However, in practice this can also lead to degradations, especially in receivers with automatic gain control.

For multiple-channel systems the interactions are more complicated but qualitatively similar. In general, the longer-wavelength channels will be amplified at the expense of the shorter-wavelength channels. The degradation can be estimated [18] by assuming that the Raman gain profile (Fig. 1) between 0 and 500 cm^{-1} is triangular. The result is that in a system of N channels with channel spacing Δf and power P per channel, no channel will experience a 1-dB penalty provided

$$[NP]\,[(N - 1)\Delta f] < 500\ \text{GHz} \cdot \text{W}. \qquad (5)$$

Note that NP is the total optical power injected into the fiber and $(N - 1)\,\Delta f$ is the total occupied optical bandwidth. Therefore, (5) is a very general result: the product of *total power* and *total optical bandwidth* must be smaller than 500 GHz · W to reduce degradation due to SRS to acceptable levels.

All the SRS results can be summarized assuming the system parameters in Section II. Fig. 3 shows the maximum allowable power *per channel* as a function of number of channels. For several channels the power limit decreases as $1/N$ because the Raman gain profile is extremely broad and the powers in all N channels contribute to the SRS process (see (4)). As more channels are added, the occupied optical bandwidth increases and the interchannel interactions become more significant and the maximum power per channel decrease as $1/N^2$ (see (5)). These results have been derived assuming equal group ve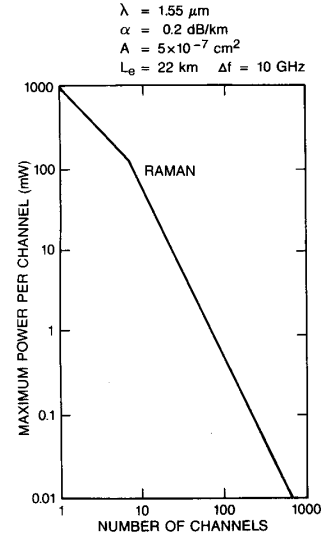locities. It has been shown [19] that the effect of group velocity dispersion on the nonlinear Raman interaction decreases the effect by a factor between 1 and 2. For high bit rates and nonzero group velocity dispersion the effects of SRS are reduced by a factor of 2. Consequently, the curve in Fig. 3 will be 3 dB higher in power.

These results were derived assuming there is optical power in every channel. In wavelength-multiplexed amplitude-shift-keyed (ASK) systems with many channels, the probability of marks occurring in all channels is small and statistical considerations must be employed. The overall Raman degradation will be reduced by occurrence of spaces in some channels. In frequency-shift-keyed (FSK) and phase-shift-keyed (PSK) systems the optical power in each channel is nominally constant and statistical treatment is not needed.

SRS arises from a third-order nonlinear susceptibility which has a subpicosecond time constant. Since this is essentially instantaneous compared to modulation rates in lightwave systems, SRS effects will be the same for both modulated and continuous wave (CW) light.

IV. CARRIER-INDUCED PHASE MODULATION

In phase-shift-keyed systems information is digitally impressed on the phase of the wave, typically toggling between $+ (\pi/2)$ and $- (\pi/2)$ to represent a logic "1" and a logic "0". Any source of phase noise in such systems will degrade system performance. An example of an optical nonlinearity that affects only the phase of the propagating signal is the nonlinear refractive index of the fiber material, which gives rise to carrier-induced phase modulation (CIP) [20]. In single-channel configurations CIP is called self-phase modulation and converts optical power fluctuations in a light wave to phase fluctuations in the same wave. In wavelength-multiplexed systems cross-

phase modulation converts power fluctuations in a particular channel to phase fluctuations in the other channels.

CIP in silica fibers exists because of an intensity-dependent refractive index. The refractive index of most transparent solids, including silica, has the form

$$n = n_o + n_2 I \qquad (6)$$

where n_o is the ordinary refractive index associated with the material, n_2 is the intensity-dependent refractive index, and I is the optical intensity (P/A). Consequently the phase of light after propagating through a fiber with length L (relative to the phase of the injected light) is

$$\phi(L) = \frac{2\pi n_o L}{\lambda} + \frac{2\pi n_2 I L_e}{\lambda}. \qquad (7)$$

Clearly, any changes in optical intensity I will produce corresponding changes in the phase and can potentially impact PSK systems. In silica for self-modulation $n_2 = 3 \times 10^{-16}$ cm^2/W and for cross-phase modulation $n_2 = 6 \times 10^{-16}$ cm^2/W [4]. Although these are very small refractive indexes the long interaction lengths in optical fibers magnify these effects.

Using (7) and accounting for random polarization [21] it can be shown that in single-channel systems the phase change in the received signal due to the nonlinear refractive index is given by

$$\sigma_\phi = 0.035\sigma_p \qquad (8)$$

where σ_ϕ is the rms phase fluctuation in radians and σ_p is the rms power fluctuation in milliwatts.

Power fluctuations in InGaAsP injection lasers are quite small [22], and increase roughly as the square root of the optical power [23]. Even for transmitter powers up to 100 mW the power fluctuations σ_p will be less than 1 mW. (We assume that the bandwidth of the power fluctuations is comparable to or less than the information bandwidth of the transmission system. This is a reasonable approximation for data rates in the gigabit-per-second range.) The resultant phase noise is less than 0.04 rd, which is negligibly small in angle-modulated systems [24] (0.15 rd of phase noise corresponds to a power penalty of roughly 0.5 dB).

In wavelength-multiplexed systems, in addition to self-phase modulation, there are cross-phase modulation effects due to power fluctuations in other optical channels. In a system with N channels, the rms phase fluctuations in a particular channel due to power fluctuations in the other channel is

$$\sigma_\phi = 0.07 \sqrt{N}\sigma_p \qquad (9)$$

where σ_ϕ is in radians and σ_p is in milliwatts. The power fluctuations σ_p in all the channels have been assumed to be the same. Assuming the laser noise characteristics just described, the limitations due to CIP will be negligible even for large numbers of channels.

Much larger CIP can be generated from residual AM present when semiconductor lasers are directly phase
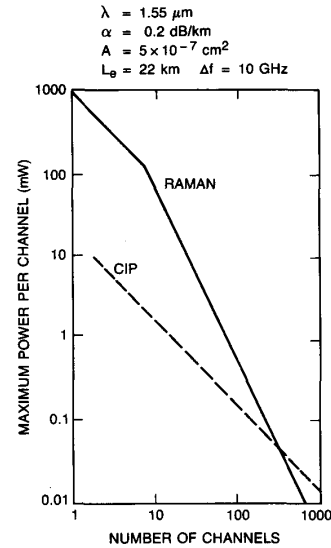

Fig. 4. Maximum power per channel versus number of channels which ensures degradations due to SRS and CIP below 1 dB for all channels. The CIP curve is for directly phase-modulated lasers with 20% residual AM.

modulated [25]. Residual AM as large as 20% of the laser output power are typical [25]. Furthermore, the degradation in this case grows linearly with N rather than as $\sqrt{N}$ [20]. In order to limit power penalties due to CIP to less than 1 dB the power per channel (assuming 20% residual AM) must satisfy

$$P < \frac{21}{N}. \qquad (10)$$

This requirement is plotted in Fig. 4. For comparison the Raman results are included.

As in the case of SRS, a third-order electric susceptibility gives rise to CIP. Consequently, this is essentially an instantaneous effect and the results apply to both CW and modulated lightwaves. Similarly the CIP results in Fig. 4 assume marks or spaces in all channels. For large number of channels statistical occurrences of marks and spaces will change the results by a small factor.

V. STIMULATED BRILLOUIN SCATTERING

Superficially, stimulated Brillouin scattering (SBS) [26] is similar to SRS except that SBS involves sound waves rather than molecular vibrations. In this respect, both scattering processes are three-wave processes in which the incident (pump) light is converted into (Stokes) light of longer wavelength with a concomitant excitation of a molecular vibration (SRS) or an acoustic phonon (SBS). However, there is a number of significant differences between SBS and SRS that lead to markedly different systems consequences.

First, the peak SBS gain coefficient in single-mode fibers is over two orders of magnitude larger ($g_B \approx 4 \times 10^{-9}$ cm/W [3]) than the gain coefficient for SRS and

approximately wavelength independent. Consequently, under the proper conditions SBS will be the dominant nonlinear process. Second, the optical-gain bandwidth $\Delta \nu_R$ for SRS is on the order of 200 cm^{-1} FWHM (6000 GHz). Therefore, there is essentially no reduction in Raman gain for pump lasers with large linewidths. The optical bandwidth $\Delta \nu_B$ for SBS in silica, on the other hand, is about 20 MHz at 1.55 μm [27] and varies as λ^{-2} [5]. (The actual bandwidth in single-mode fibers can vary from 20 to about 100 MHz depending on fiber geometry and compositional effects, but for the purposes of this discussion a 20-MHz bandwidth is assumed.) Maximum SBS gain will occur for pump lasers with linewidths less than 20 MHz. For lasers with linewidths $\Delta \nu_L$ much larger than 20 MHz, SBS gain decreases as the ratio $\Delta \nu_B / \Delta \nu_L$, that is, $g = g_B \Delta \nu_B / \Delta \nu_L$ [3], where g_B is the maximum steady-state Brillouin gain. Unlike SRS, which can occur in co-propagating or counterpropagating geometries, SBS (due to phase-matching considerations) occurs only in the backward direction in single-mode fibers. This process obviously depletes the incident wave, and, in addition, generates a potentially strong scattered beam propagating back toward the transmitter [3], [13]. The scattered light is shifted to a lower frequency by an amount $f_B = 2nV_s / \lambda$, where n is the refractive index, and V_S is the velocity of sound in the fiber. At 1.55 μm $f_B \approx 11$ GHz for silica glasses.

In a single channel the critical power level at which SBS degrades system performance is [1]

$$P_c = 21b\, A_e / (g_B L_e). \qquad (11)$$

For the previously assumed system parameters $P_c = 2.4$ mW. In multichannel systems it can be shown [28], [29] each channel interacts with the fiber independent of other channels. Consequently the critical power is constant with increasing number of channels (Fig. 5).

The above results have been derived assuming CW signal waves. Unlike SRS and CIP, SBS is very sensitive to signal modulation because the origin of SBS involves a process which, unlike nuclear susceptibilities, is not instantaneous on the time scale of the information rate. The acoustic phonons which scatter light have long lifetimes, as evidenced by the narrow Brillouin linewidths (20 MHz). High modulation rates produce broad optical spectra and a reduction in stimulated Brillouin amplification can be expected. The analysis developed for SBS generated by a narrow-linewidth source [30] can be extended [28], [29] to multimode sources and finally to sources with pseudorandom modulation [31] used in communications. The results depend on the particular encoding scheme used: ASK, FSK, PSK, and on the ratio $B / \Delta \nu_B$ where B is the bit rate.

For nonreturn-to-zero ASK, the launched field amplitude can be described by

$$E(t) = E_O \left(1 - [1 - m(t)] \left[1 - (1 - k_a)^{1/2}\right] \right) \qquad (12)$$

where the binary data stream is represented by the function $m(t)$ that can take values of 0 and 1 with equal prob-
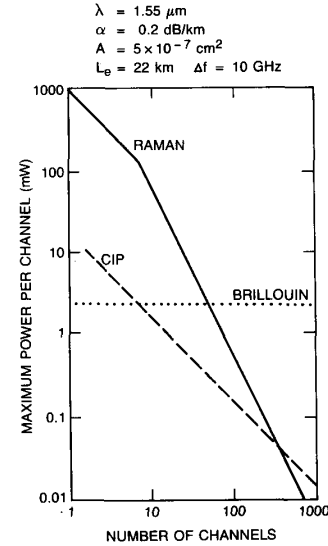

Fig. 5. Maximum power per channel versus number of channels which ensures SRS, CIP, and SBS degradations below 1 dB for all channels. The SBS curve assumes CW power.

ability, and k_a is the depth of intensity modulation ($0 < k_a \leq 1$). In this case the SBS gain is [31]

$$g = g_B \left[\left(1 - \frac{a}{2}\right)^2 + \frac{a^2}{4}\left(1 - \frac{B}{\Delta \nu_B}\left(1 - e^{-\Delta \nu_B / B}\right)\right) \right] \qquad (13)$$

where $a = 1 - (1 - k_a)^{1/2}$. In actual systems the carrier spike might be broadened by pattern dependent FM response common in injection lasers. This will cause a further decrease in SBS gain.

The SBS gain for ASK can be minimized by using a 100% modulation depth ($k_a = 1$). For bit rates much smaller than the Brillouin linewidth g approaches $g_B / 2$. For high bit rates g approaches $g_B / 4$. The dependence of g on $B / \Delta \nu_B$ is summarized in Fig. 6.

In PSK, the information is impressed on the phase of the electric field, as given by

$$E(t) = E_o e^{i\phi(t)} \qquad (14)$$

where $\phi(t) = k_p m(t)$ and k_p is the keyed phase shift. The SBS gain for PSK is [31]

$$g = g_b \left[\frac{1}{2}\left(1 + \cos k_p\right) + \frac{1}{2}\left(1 - \cos k_p\right)\left[1 - \frac{B}{\Delta \nu_B}\left(1 - e^{-\Delta \nu_B / B}\right)\right]\right]. \qquad (15)$$

The gain for PSK is minimized for $k_p = \pi(2n + 1)$, i.e., suppressed carrier. For high bit rates the SBS gain decreases linearly with $B / \Delta \nu_B$ (Fig. 6).

In wide-deviation FSK modulation the laser frequency is modulated between two relatively widely spaced frequencies ω_1 and ω_2, that is the modulation depth $k_f = \omega_1$
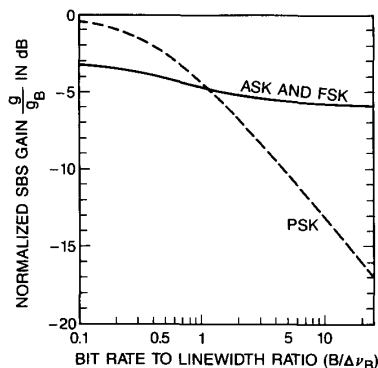
Fig. 6. Normalized SBS gain as a function of the ratio of bit rate to Brillouin linewidth (from [31]).

Fig. 7. Four-photon mixing with two injected waves at frequencies f_1 and f_2.

Fig. 8. Four-photon mixing with three injected waves at frequencies f_1, f_2, and f_3. The generated frequencies $f_{ijk} = f_i + f_j - f_k$.

$- \omega_2$ is at least several times the bit rate B. Consequently, the FSK spectrum is just the sum of two ASK spectra with $k_a = 1$ centered about ω_1 and ω_2. Therefore, the SBS gain for FSK is simply

$$g = g_B \left[\frac{1}{2} - \frac{B}{4\Delta \nu_B} \left(1 - e^{-B/\Delta \nu_B} \right) \right]. \qquad (16)$$

As shown in Fig. 6, the dependence of g on $B/\Delta \nu_B$ for FSK is the same as ASK. At high bit rates the SBS gain decreases from the CW value by a factor of 4.

To summarize, SBS is a very strong nonlinear process that exhibits gain in the backward direction. This nonlinearity is most detrimental in systems employing narrow-bandwidth lasers. In general, encoding pseudorandom data on the optical wave will reduce the effects of SBS. Maximum reduction occurs by using 100% modulation depth ($k_a = 1$) in ASK systems and $k_p = \pi(2n + 1)$ in PSK systems. The SBS gain decreases with increasing bit rates. In ASK and FSK systems the maximum reduction is a factor of 4. For high-bit-rate PSK systems the SBS gain decreases linearly with B.

An additional observation needs to be made about SBS in ASK systems. The discussion above assumes an information-rate-limited signal, i.e., a signal produced by an externally modulated laser. Directly modulated lasers typically have a chirped spectrum many gigahertz wide. This will greatly reduce the SBS gain coefficient. To maintain SBS gains given by (13) there must be a clearly defined narrow (<20 MHz) carrier in the modulated signal. Such a carrier is typically absent in directly modulated semiconductor lasers.

VI. FOUR-PHOTON MIXING

The same nonlinearity that gives rise to the nonlinear refractive index also mediates the four-photon mixing process in single-mode fibers [2]. The simplest embodiment of this effect is shown in Fig. 7. Two copropagating waves at frequencies f_1 and f_2 mix and generate sidebands at $2f_1 - f_2$ and $2f_2 - f_1$. These sidebands copropagate with the initial waves and grow at their expense. Similarly, three copropagating waves will generate nine new optical waves (Fig. 8) at frequencies $f_{ijk} = f_i + f_j - f_k$
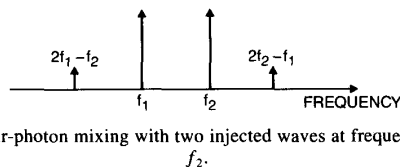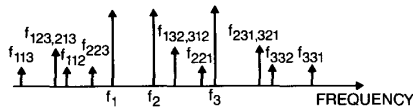
where i, j, and k can be 1, 2, or 3. If the channels are equally spaced, some of the generated waves will have the same frequencies as the injected waves. Clearly the appearance of the additional waves as well as the depletion of the initial waves will degrade multichannel systems by crosstalk or excess attenuation.

The efficiency of four-photon mixing depends on the channel spacing and the fiber dispersion. Because of fiber chromatic dispersion the interacting and generated waves have different group velocities. This destroys the phase matching of the interacting waves and lowers the efficiency of power generation at new frequencies [2], [32]. The four-photon mixing efficiency decreases with increasing group velocity mismatch. Consequently larger channel spacing and greater group velocity dispersion lead to lower efficiencies. The power P_{ijk} (L) exiting the fiber generated at frequency f_{ijk} due to the interaction of channels at frequencies f_i, f_j, and f_k is [2], [32] (in cgs/esu units)

$$P_{ijk}(L) = \eta \left(1024\pi^6/n^4\lambda^2 c^2 \right) \left(D\chi_{1111} \right)^2 \left(L_e/A_e \right)^2$$
$$\times P_i P_j P_k \exp \left(-\alpha L \right) \qquad (17)$$

where χ_{1111} is the third-order nonlinear susceptibility ($\chi_{1111} = 6 \times 10^{-15}$ cm^3/erg), η is the efficiency of four-photon mixing, and $D = 3$ or 6 for two waves mixing (Fig. 7) or three waves mixing (Fig. 8), respectively. An explicit expression for η can be found in [32] but two specific examples in Fig. 9 are enough to gain some insight. The generation efficiency is plotted as a function of channel separation for two values of dispersion. The solid curve is the efficiency for the dispersion of a conventional single-mode fiber, 16 ps/nm · km. The dashed curve is the efficiency for dispersion-shifted fiber with a dispersion of 1 ps/nm · km. These plots show the frequency range over which the four-photon mixing process is efficient. For example, in the conventional fiber only channels with separations less than 20 GHz will mix efficiently. On the other hand, in dispersion-shifted fibers four-photon mixing efficiencies are greater than 20% for channel separations up to 50 GHz. Equation (17) and Fig. 9 can now be used to determine the four-photon mixing limitations in
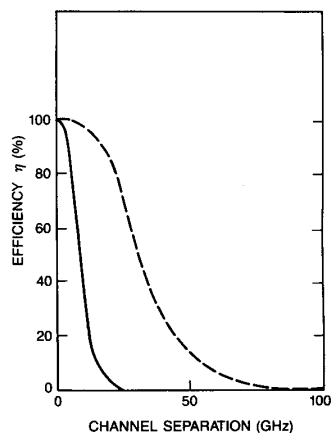
Fig. 9. Four-photon mixing efficiency as a function of channel separation at 1.55 μm. The solid curve represents standard single-mode fiber with dispersion equal 16 ps/nm · km. The dashed curve is for dispersion-shifted fiber with dispersion of 1 ps/nm · km.
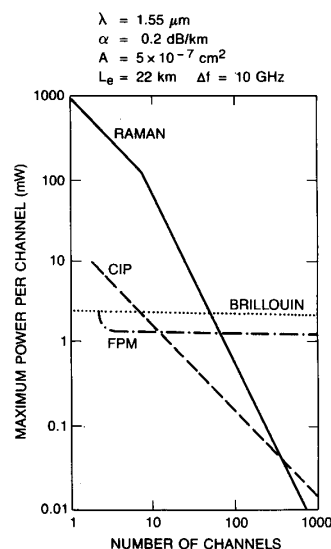

Fig. 10. Maximum power per channel versus number of channels which ensures SRS, CIP, SBS, and FPM degradations below 1 dB for all channels.

lightwave systems. With system parameters assumed previously, Fig. 10 shows the maximum power per channel that can be transmitted without degradation by four-photon mixing. The slight curvature at the small channel number indicates that the four-photon interaction occurs between a channel and its two closest neighbors as determined by Fig. 9.

Because the FPM nonlinearity couples nearby channels and does not have the frequency extent of SRS and CIP statistical occurrence of marks in ASK systems need not be considered. As for SRS and CIP, the effects of FMP are bit-rate independent.
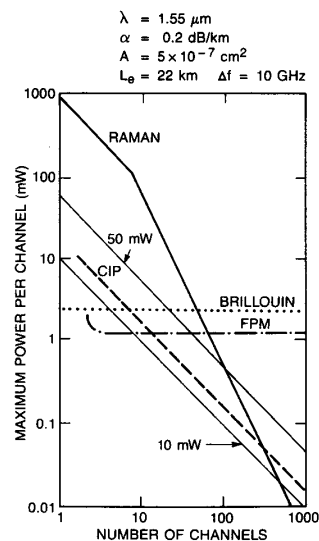

Fig. 11. Same as Fig. 10 but including curves for the power per channel injected into the fiber assuming lossless passive multiplexing for 10- and 50-mW lasers.

VII. MULTIPLEXING EFFECTS

Different methods of multiplexing (passive versus frequency-selective) impact dramatically on the effects of optical nonlinearities. Passive multiplexing of N channels by a star coupler, for example, reduces the power per channel injected into the fiber by a factor N. Higher degrees of multiplexing lead to lower powers per channel injected into the fiber. Multiplexing followed by semiconductor amplifiers will not change the situation because the saturation power of semiconductor amplifiers is about the same as the output power of an injection laser. Therefore, the power per channel injected into the fiber using passive multiplexing decreases with channel number as shown in Fig. 11 for 10- and 50-mW laser transmitters (assuming no excess multiplexing loss). A particular nonlinearity will cause system degradation if the curve associated with that nonlinearity in Fig. 11 lies below the line representing the system transmitter power. For the case of frequency-selective multiplexing the power per channel injected into the fiber will be independent of channel number. Consequently, such systems will be more susceptible to degradations by optical nonlinearities.

VIII. SCALING

The effect of changes in system parameters on the limitations due to optical nonlinearities is straightforward for SRS, CIP, and SBS. Scaling laws for four-photon mixing are complicated by the complex dependence of the mixing efficiency η on system parameters [32]. The system parameters which affect the nonlinear optical effects are fiber attenuation coefficient α, fiber core area A_e, chromatic dispersion, channel separation, fiber polarization properties, and strength of nonlinear gain processes g.
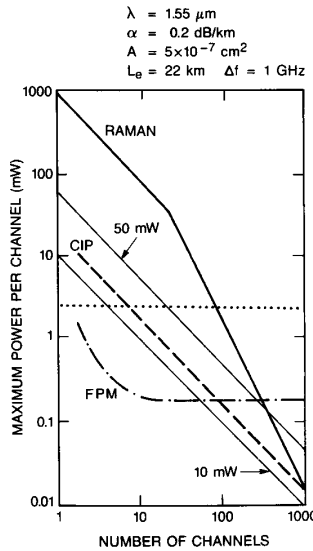
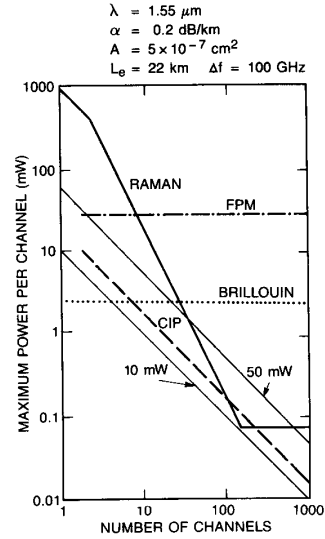Fig. 12. Same as Fig. 11 but for 1-GHz channel spacing.

Fig. 13. Same as Fig. 11 but for 100-GHz channel spacing.

SRS, CIP, and SBS scale with the ratio gL_e/bA_e. Changing fiber loss or fiber length changes L_e given by (3). Polarization maintaining fibers will increase the nonlinear effect by a factor of 2. The dependence on core area is obvious. Similarly if the strength of the nonlinearity g is changed (for example, in the case of mid-infrared fibers with different material compositions), the effects of the nonlinearity will scale proportionately. Four-photon mixing depends on system parameters in a more complicated way and needs to be evaluated for each case. The dependence of nonlinear effects on channel separation is straightforward. For CIP and SBS the effects are independent of channel spacing. For SRS the effects are directly related to channel spacing (total occupied optical bandwidth, (5)). In this case, decreasing channel spacing reduces SRS because of the nearly triangular shape of the Raman gain. The opposite is true for FPM. In this case, decreasing channel spacing allows each channel to interact with more neighboring channels (Fig. 9) thereby increasing the nonlinear effects. Figs. 12 and 13 are two examples of dependence of nonlinear effects on channel spacing. For 1-GHz channel separation (Fig. 12) the effects of SRS are diminished whereas the effects of FPM are enhanced compared to 10-GHz channel spacing. Note the added curvature in the FPM plot indicates the increased extent of channel interaction. SBS and CIP curves are unaltered. For 100-GHz channel separation (Fig. 13) the effects of SRS are enhanced (total occupied bandwidth is larger). The break in the SRS curve at about channel number 150 indicates the total occupied optical bandwidth is equal to the Raman width as approximated by a triangular profile. Adding more channels does not further degrade the system. The effects of FPM mixing are dramatically reduced because the FPM coefficient is small. Again, CIP and SBS are unaffected.

IX. EXPERIMENTS

Optical nonlinearities in silica fibers have been widely studied experimentally. Several experimental studies of each nonlinearity will be summarized in this section. Generally, the experimental results agree remarkably well with theoretical predictions.

The effects of SRS in two-channel configurations have been measured in several ways [33]-[35]. The crosstalk due to SRS was measured [34] using light from two injection lasers multiplexed on a fiber 21-km long. The power in the long-wavelength channel (1.34 μm) was deliberately reduced to 0.05 mW to avoid depletion of the short-wavelength channel (1.26 μm). Thus, the effects of SRS were monitored not by measuring the degradation of the short-wavelength channel but by measuring the amplification of the long-wavelength channel as a function of power in the short-wavelength channel. Both continuous wave (CW) and modulated (230-MHz square wave) signals were employed. For 1 mW of power at 1.26 μm a crosstalk of -25 dB was measured, in good agreement with theoretical prediction.

The degradation of a short-wavelength channel due to depletion by a long-wavelength channel in a two-channel configuration was measured directly by determining power penalties from bit-error-rate (BER) curves [35]. Light from a DFB injection laser operating at 1.5 μm was transmitted through 43 km of fiber. The laser was modulated with a $2^{15} - 1$ pseudorandom bit stream at 1 Gb/s, and the BER was measured as a function of received power. Light from a color-center laser (FCL) emitting up to 150 mW at 1.57 μm was then also injected into the fiber and the BER curves were measured for several FCL powers. The BER measurements displayed power penalties up to 2.5 dB. The measured power penalties corresponded to the observed depletion levels in the short-wavelength channels and agreed with the predicted degradations.

In a wavelength-multiplexing experiment [36], ten channels occupying a total optical bandwidth of 30 nm were multiplexed on a 68-km long fiber. The average total injected power in all channels was about 5 mW. Therefore, total power × optical bandwidth = 20 GHz · W, well below the figure needed to produce an observable penalty (see (5)). Indeed, no power penalty due to SRS was observed in the BER measurements.

Cross-phase modulation has been experimentally observed using light from two conventional InGaAsP injection lasers multiplexed on a 15-km-long single-mode fiber [37]. In the experiment to measure the effects of cross-phase modulation, a novel self-reflexive interferometer was employed. The channel 1 source was a CW 1.5-μm InGaAsP single-frequency distributed-feedback laser with a coherence length of several meters, and channel 2 used a 1.3-μm InGaAsP V-groove buried-crescent multifrequency laser. The two beams were combined by a dichroic mirror and coupled into a 15-km-long depressed-step-index single-mode fiber. The effects of ON–OFF modulation in channel 2 on the phase of the CW light in channel 1 were measured. A 1-mW change in the power of channel 2 produced a 0.024-rd phase shift in channel 1. The predicted value is 0.022 rd.

SBS has been observed in numerous experiments [38], [39] and as fiber loss was reduced, SBS thresholds approaching 2 mW were observed at a 1.52 μm in 30-km-long fiber [40]. The effects on SBS thresholds of multiple frequencies were recently studied [29], [41] and the SBS gain reduction due to pump modulation predicted in Fig. 6 was confirmed [31], [42].

Several FPM experiments at different wavelengths have supported theoretical predictions. Two experiments [32], [43] used 0.8-μm-wavelength lasers where fiber dispersion is on the order of 100 ps/nm · km. More recently, [44] experiments in dispersion-shifted fibers using 1.3- and 1.55-μm sources have confirmed the dependence of FPM efficiency on channel spacing and fiber dispersion.

X. CONCLUSIONS

Of the four nonlinearities, SRS is least likely to affect lightwave systems. Only in wavelength multiplexed systems with hundreds of channels will SRS contribute to system degradations.

Carrier-induced phase noise is not a significant nonlinearity in PSK systems using external phase modulators. Directly phase-modulated lasers, however, have residual AM which can cause phase fluctuations detrimental to PSK systems. Even in passively multiplexed systems lasers above about 20 mW in power will cause degradations. In frequency-selective-multiplexed systems, even low power lasers (several milliwatts) will be unacceptable for systems with more than ten channels.

The effects of SBS are directly related to transmitter power and independent of number of channels. Consequently, SBS will degrade passively multiplexed systems with few channels more readily than systems with many channels. As usual, frequency-selective multiplexing ex-

acerbates the effects of the nonlinearity. For typical high-speed, long-haul systems transmitter powers exceeding 10 mW will degrade system performance.

Of all the nonlinearities FPM is the most sensitive to system parameters. Not only does it depend on fiber length and core area but it also depends on channel separation and fiber dispersion. To reduce the effects of FPM channel separations should be greater than about 50 GHz, and the wavelength region of minimum dispersion should be avoided. For standard fibers (dispersion zero at 1.3 μm) and channel separations of a few tens of gigahertz, FPM will degrade multiplexed systems for transmitter powers of a few milliwatts.

The system implications of optical nonlinearities can be described by plots such as Figs. 11–13. For each nonlinearity a curve shows the maximum allowable power per channel in order to restrict the worst-case power penalty due to that nonlinearity to less than 1 dB. The actual optical powers injected into the system can then be superposed on these plots. For passive multiplexing these powers will decrease as $1/N$ with increasing number of channels (examples for 10- and 50-mW lasers are shown in Figs. 11–13). For frequency-selective multiplexing the transmitter powers will be represented by a horizontal line. Existence of system degradations due to a particular nonlinearity can be identified by locating regions where the curve representing that nonlinearity lies below the line representing the system transmitter power. Except for SBS these results are independent of bit-rate. For SBS, bit rates larger than about 100 Mb/s will decrease the effects of the nonlinearity as discussed in Section V.

REFERENCES

[1] R. G. Smith, "Optical power handling capacity of low-loss optical fibers as determined by stimulated Raman and Brillouin scattering,"*Appl. Opt.*, vol. 11, p. 2489, 1972.

[2] K. O. Hill, D. C. Johnson, B. S. Kawasaki, and R. I. MacDonald, "CW three-wave mixing in single-mode optical fibers," *J. Appl. Phys.*, vol. 49, p. 5098, 1978.

[3] R. H. Stolen, "Nonlinear properties of optical fibers," in *Optical Fiber Telecommunications*, S. E. Miller and A. G. Chynoweth, Eds. New York: Academic, 1979, p. 130.

[4] R. H. Stolen and J. E. Bjorkholm, "Parametric amplification and frequency conversion in optical fibers," *IEEE J. Quantum Electron.*, vol. QE-18, pp. 1062–1072, 1982.

[5] D. C. Johnson, K. O. Hill, and B. S. Kawasaki, *Radio Si.*, vol. 12, p. 519, 1977.

[6] N. Bloembergen, "The stimulated Raman effect," *Am. J. Phys.*, vol. 35, p. 989, 1967.

[7] W. Kaiser and M. Maier, "Stimulated Rayleigh, Brillouin and Raman spectroscopy," in *Laser Handbook*, F. T. Arecchi and E. O. Schulz-Dubois, Eds. Amsterdam: North-Holland, p. 1077.

[8] A. Yariv, *Quantum Electronics*, 2nd ed. New York: Wiley, 1975.

[9] B. P. Stoicheff, "Characteristics of stimulated Raman radiation generated by coherent light," *Phys. Lett.*, vol. 7, p. 186.

[10] R. Shuker and R. W. Gammon, "Raman-scattering selection-rule breaking and the density of states in amorphous materials," *Phys. Rev. Lett.*, vol. 25, p. 222, 1970.

[11] R. H. Stolen and E. P. Ippen, "Raman gain in glass optical waveguides," *Appl. Phys. Lett.*, vol. 22, p. 276, 1973.

[12] J. Auyeung and A. Yariv, "Spontaneous and stimulated Raman scattering in long low-loss fibers," *IEEE J. Quantum Electron.*, vol. QE-14, p. 347, 1978.

[13] R. H. Stolen, "Nonlinearity in fiber transmission," *Proc. IEEE*, vol. 68, p. 1232, 1980.

[14] Y. Ohmori, Y. Sasaki, M. Kawachi, and T. Edahiro, "Fibre-length dependence of critical power for stimulated Raman scattering," *Electron. Lett.*, vol. 17, p. 593, 1981.

[15] M. Ikeda, "Spectral power handling capability caused by stimulated Raman scattering effect in silica optical fiber," *Opt. Commun.*, vol. 37, p. 388, 1981.

[16] R. H. Stolen, Clinton Lee, and R. K. Jain, "Development of the stimulated Raman spectrum in single-mode silica fibers," *J. Opt. Soc. Amer. B.*, vol. 1, p. 652, 1984.

[17] A. R. Chraplyvy and P. S. Henry, "Performance degradation due to stimulated Raman scattering in wavelength-division-multiplexed optical-fibre systems," *Electon. Lett.*, vol. 19, p. 641, 1983.

[18] A. R. Chraplyvy, "Optical power limits in multichannel wavelength-division-multiplexed systems due to stimulated Raman scattering," *Electron. Lett.*, vol. 20, p. 58, 1984.

[19] D. Cotter and A. M. Hill, "Stimulated Raman crosstalk in optical transmission: Effects of group velocity dispersion," *Electron. Lett.*, vol. 20, p. 85, 1984.

[20] A. R. Chraplyvy, D. M. Marcuse, and P. S. Henry, "Carrier-induced phase noise in angle-modulated optical-fiber systems," *J. Lightwave Technol.*, vol. LT-22, p. 6, 1984.

[21] R. H. Stolen and C. Lin, "Self-phase modulation in silica optical fibers," *Phys. Rev. A.*, vol. 17, p. 1448, 1978.

[22] P-L. Liu, J-S Ko, I. P. Kaminow, T. P. Lee, and C. A. Burrus, "Steady-state intensity fluctuations, photon statistics and mode partitioning of injection lasers," in *Tech. Dig. Sixth Topical Meet. Opt. Fiber Comm.* (New Orleans, LA), 1983, paper PD-3.

[23] Y. Yamamoto, S. Saito, and T. Mukai, "AM and FM quantum noise in semiconductor lasers—Part II," *IEEE J. Quantum Electron.*, vol. QE-19, p. 47, 1983.

[24] V. K. Prabhu, "PSK performance with imperfect carrier phase recovery," *IEEE Trans. Aero. Elect. Syst.*, vol. AES-12, p. 275, 1976.

[25] R. S. Vodhanel, "5 Gbit/s direct optical differential phase-shift keying modulation of a 1530-nm distributed-feedback laser," *Opt. Fiber Conf.*, Houston, TX, 1989.

[26] E. P. Ippen and R. H. Stolen, "Stimulated Brillouin scattering in optical fibers," *Appl. Phys. Lett.*, vol. 21, p. 539, 1972.

[27] D. Heiman, D. S. Hamilton, and R. W. Hellwarth, "Brillouin scattering measurements on optical glasses," *Phys. Rev.*, vol. B19, p. 6583, 1979.

[28] Y. Aoki and K. Tajima, "Dependence of the stimulated Brillouin scattering threshold in single-mode fibers on the number of longitudinal modes of a pump laser," in *Tech. Dig., Conf. Lasers and Electrooptics* (Baltimore, Md), 1987, paper Tu HH5.

[29] E. Lichtman and A. A. Friesem, "Stimulated Brillouin scattering excited by a multimode laser in single-mode optical fibers," *Opt. Comm.*, vol. 64, p. 544, 1987.

[30] C. L. Tang, "Saturation and spectral characteristics of the Stokes emission in the stimulated Brillouin process," *J. Appl. Phys.*, vol. 37, p. 2945, 1966.

[31] E. Lichtman, R. G. Waarts, and A. A. Friesem, "Stimulated Brillouin scattering excited by a modulated pump wave in single-mode fibers," *J. Lightwave Technol.*, vol. 7, p. 171, 1989.

[32] N. Shibata, R. P. Braun, and R. G. Waarts, "Phase-mismatch dependence of efficiency of wave generation through four-wave mixing in a single-mode optical fiber," *IEEE J. Quantum Electron.*, vol. QE-23, p. 1205, 1987.

[33] M. Ikeda, "Stimulated Raman amplification characteristics in long span single-mode silica fibers," *Opt. Comm.*, vol. 39, p. 148, 1981.

[34] A. Tomita, "Crosstalk caused by stimulated Raman scattering in single-mode wavelength-division multiplexed systems," *Opt. Lett.*, vol. 8, p. 412, 1983.

[35] J. Hegarty, N. A. Olsson, and M. McGlashan-Powell, "Measurement of the Raman crosstalk at 1.5 μm in a wavelength-division-multiplexed transmission system," *Electron. Lett.*, vol. 21, p. 395, 1985.

[36] N. A. Olsson *et al.*, "68.3-km transmission with 1.37 Tbitkm/sec capacity using wavelength-division-multiplexing of ten single-frequency lasers at 1.5 μm," *Electron Lett.*, vol. 21, p. 105, 1985.

[37] A. R. Chraplyvy and J. Stone, "Measurement of crossphase modulation in coherent wavelength-division multiplexing using injection lasers," *Electron. Lett.*, vol. 20, p. 996, 1984.

[38] N. Uesugi, M. Ikeda, and Y. Sasaki, "Maximum single-frequency input power in a long optical fiber determined by stimulated Brillouin scattering," *Electron. Lett.*, vol. 17, p. 379, 1981.

[39] D. Cotter, "Observation of stimulated Brillouin scattering in low-loss silica fibre at 1.3 μm," *Electron. Lett.*, vol. 18, p. 495, 1982.

[40] D. Cotter, "Optical nonlinearity in fibers: A new factor in systems design," *Brit. Telecommun. Technol. J.*, vol. 1, p. 17, 1983.

[41] Y. Aoki and K. Tajima, "Stimulated Brillouin scattering in a long single-mode fiber excited with a multimode pump laser," to be published in *J. Opt. Soc. B.*.

[42] Y. Aoki, K. Tajima, and I. Mito, "Input power limits of single-mode optical fibers due to stimulated Brillouin scattering in optical communication systems," *J. Lightwave Technol.*, vol. 6, p. 710, 1988.

[43] N. Shibata, R. P. Braun, and R. G. Waarts, "Crosstalk due to three-wave mixing process in a coherent single-mode transmission line," *Electron. Lett.*, vol. 22, p. 675, 1986.

[44] N. Shibata, Y. Azuma, M. Tateda, and Y. Nakamo, "Experimental verification of efficiency of wave generation through four-wave mixing in low-loss dispersion-shifted single-mode optical fiber," *Electron. Lett.*, vol. 24, p. 1528, 1988.

Andrew R. Chraplyvy, photograph and biography not available at the time of publication.